ANALYSIS OF HUMAN RECEPTOR DENSITY

CHRISTOPHER W. TYLER
Smith-Kettlewell Eye Research Institute,
2232 Webster St., San Francisco CA 94115

Abstract

Data for densities and sizes of human cones were analyzed as a function of retinal eccentricity. Density of cones followed a decreasing power of about -2/3 over much of the eccentricity range. This decrease, and the subsequent increase in cone density toward the ora serrata, were predictable on the basis of a hypothetical density-control mechanism to equate the integrated luminous flux at the photoreceptors per unit retinal area, together with the empirical rule that cone diameter increases with a power of about 1/3 with eccentricity beyond the foveola. The analysis implies that cones aggregate in inverse proportion to the light impinging on them, and provides an explanation for the pronounced increase to 100% cone density at the ora serrata.

Introduction

Knowledge of the density of receptors as a function of retinal eccentricity is important in studies of spatial resolution, visual sensitivity and the dissection of neural contributions to the visual response. Until recently, the only extensive investigation of overall receptor density in human was by Oesterberg [1], and it has yielded a much-reproduced graph of rod and cone densities as a function of eccentricity. Oesterberg's data, which still cover the widest range of any data available on human retina, are fully validated by studies using more modern techniques [2], but there have been few attempts to characterize the data analytically or determine what principles may be operating to control the receptor distributions.

Cone distribution as a function of eccentricity: Oesterberg's complete data for cone densities in each measured location in the horizontal meridian and four retinal sectors are plotted as a function of eccentricity in double logarithmic coordinates in Fig.1. This type of plot reveals two salient characteristics of the cone distribution. First, the density falls approximately on a straight line with a slope of about -2/3 between 0.2 and 20° eccentricity, most clearly for the horizontal temporal meridian (0°) in Fig. 1 but also supported by the sparse data for the other quad-

V. Lakshminarayanan (ed.), Basic and Clinical Applications of Vision Science, 63–71.

rants. Over this range, a regression analysis of the temporal data indicates a density exponent of z=-0.63 with 99% confidence limits of ±0.022 (eq. 1).

$$d_c \propto \theta^z \qquad (1)$$

where θ is eccentricity in terms of visual angle from the fovea.

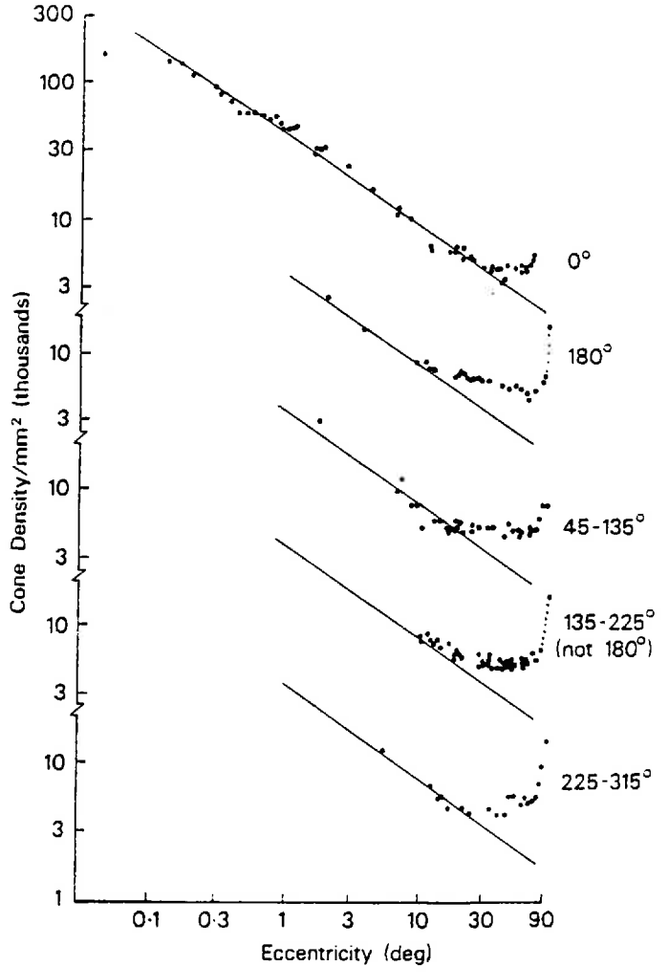

Fig. 1. Log-log plot of cone densities as a function of eccentricity for 5 retinal sectors, with successive plots displaced by 1 log unit, for a narrow sector close to the temporal (0°) meridian and nasal (180°) meridians, and for the upper, temporal and lower quadrants, respectively. Straight lines have slopes of -2/3 for comparison. Note departure of data from these functions beyond about 20° and steep rise in cone density near the ora serrata emphasized by the dotted connecting lines in two cases. From Oesterberg [1].

This confidence range strongly excludes a hyperbola with a density exponent of -1 (reciprocity between cone density and eccentricity) and also excludes a density exponent of -0.5 (reciprocity between linear cone spacing and eccentricity). For one female macaque retina, Schein [3] has similarly shown exponents with a value of -0.768 for the mean data of the four cardinal meridians and -0.771 for the temporal meridian alone, based on data out to 2.5 mm eccentricity (about 10° in visual angle).

A second point about the data of Fig. 1 is that, both in the central fovea and beyond about 20°, cone density deviates from the power function of eq. 1 and stabilizes for a large range of peripheral retina between about 20 and 60° (compressed to a small region on this logarithmic plot). In all five data sets there is, then, an increase in cone density of up to a factor of 3 as the oraserrata is reached, as noted by Oesterberg and as recently validated quantitatively by direct anatomical studies [4].

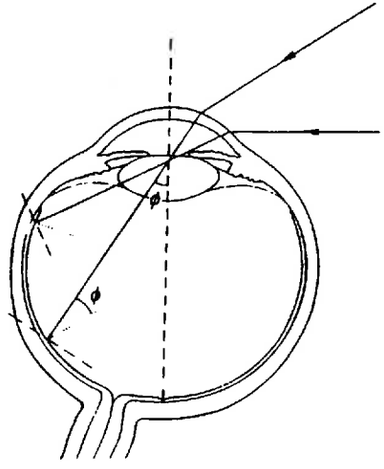

Fig. 2. Anatomic and projective geometry of the eyeball, showing oblique pupil entry for peripheral rays, projective distance to the retina, and angle of the retina relative to incident rays increasing towards the ora serrata.

Estimation of the luminous flux incident on the cones: In this section, the projective geometry for the luminous flux received by each cone with retinal eccentricity is developed as a guiding principle to explain the changes in cone density toward the ora serrata. The resulting function will be shown to be descriptive of the data in several respects, although whether this is a true functional relationship between the two will have to be determined by further comparative studies. With this proviso, it is hypothesized that the decrease in cone density with eccentricity is such as to compensate for the variation in luminous flux received by each cone. The luminous flux, F, is given simply by the product of the light-catching aperture of each cone and the retinal illuminance, L, reaching that aperture. If the

aperture of the cone corresponds to the area of the inner segment, then the incident luminous flux will be

$$F = 2 \cdot \pi \cdot r_c^2 \cdot L \qquad (2)$$

where r_c is the inner segment radius.

If the cone density is inversely proportional to luminous flux, then all that is required for a quantitative prediction is to determine the variation of the two variables, L and r_c, as a function of eccentricity. Major factors affecting the illuminance falling on the receptor as eccentricity is increased (see Fig. 2) are: (i) reduction of effective pupil area as its angle to the incident ray reduces the pupil aperture to an ellipse, and (ii) decrease in the path length to the retina causing an increase in the flux per unit retinal area.

The effective pupil area with eccentricity, and hence the incident flux, has been quantified by Spring and Stiles [5] and by Jay [6] and can be well approximated by an adjusted cosine function, as shown in Fig. 3 for Jay's data for the normal pupils of 8 observers. The approximating curve for pupil area A_p has the equation:

$$A_p = \cos(v \cdot \theta) \qquad (3)$$

where θ is the incident angle and v takes the value of 0.82.

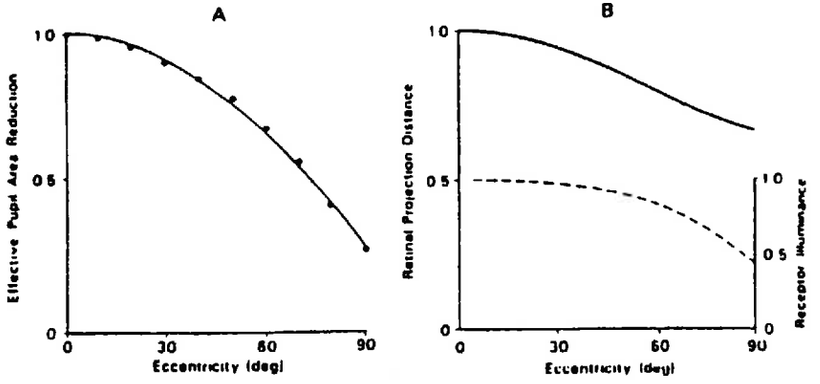

Fig 3. A. Retinal illuminance reduction as a function of eccentricity produced by oblique pupil entry. Data from Jay [6] are fitted by the cosine function of eq. 2. B. Projective distance (left ordinate; thick line) of internal rays as a function of eccentricity. Data from the wide-angle schematic model [7] are fitted by eq. 3. Dashed line and right ordinate show the reduction in receptor illuminance implied by the combination of the pupil size and projection distance functions.

The distance that the light rays have to travel to reach the retina at various eccentricities has been derived with the use of a wide-angle schematic model of the eye [7]. As the distance becomes shorter the retinal area of incident rays from a unit visual angle is reduced, with a reciprocal increase in the luminous flux per unit retinal area. The resulting estimates of the flux are shown in Fig. 3B, based on the assumption that the receptors are oriented towards the axis of the incident light [8,9]. Thus, the normalized data for optical path length, x, are fitted by the arbitrary function:

$$x = 1 - w \cdot (1 - \cos(u \cdot \theta)) \qquad (4)$$

with $w = 0.19$ and $u = \pi / 2$, as shown by the solid line in Fig. 3B. The implied receptor illuminance, L, varies with the square of this path length and with the pupil aperture from eq. 3 as given by:

$$L = A_p / x^2 \qquad (5)$$

The dashed line in Fig. 3B plots the resultant receptor illuminance function, L, which shows that the decrease in distance of the retina from the lens does not increase the illuminance sufficiently to compensate for the decreased luminous flux with pupil angle. A similar conclusion was reached by Charman [10].

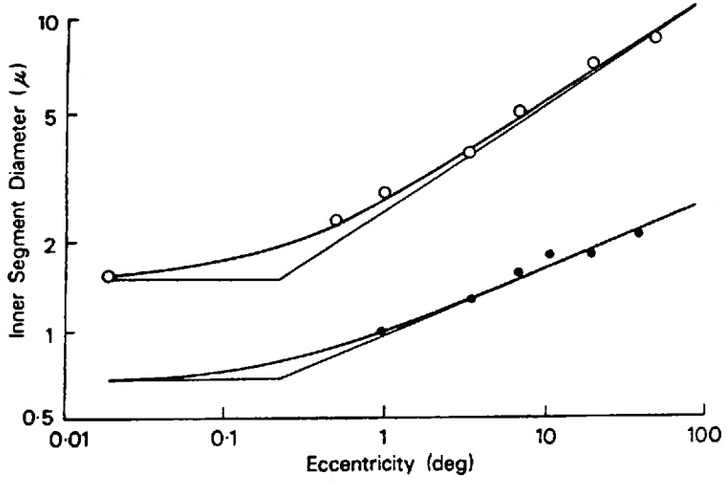

Fig. 4. Fit of function in eq. 5 to data for cone (filled circles) and rod (open circles) inner segment diameters from Polyak [8], as a function of eccentricity on double logarithmic coordinates.

The final aspect of receptor anatomy which pertains to the luminous flux impinging on each receptor is the variation in area of the inner segments with eccentricity. The most complete data available [8] for the diameter of the cone

inner segments at a range of eccentricities are shown in Fig. 4 in double logarithmic coordinates. The cone inner segments show a large increase in diameter with eccentricity (a total factor of 6), which must be taken into account for any process based on the quantum catch of each cone.

Using a similar approach to a previous analysis of these data [11], the data for cone diameters r_c are well fit by the function:

$$r_c = m_c \cdot (B+\theta)^{0.33} \qquad (6)$$

where m_c= 1.25 μ/deg and B = 0.2 deg. This function is shown as the full line in Fig. 4, and provides a good description of the data. The thin lines show the asymptotic limits of the function when θ = 0 and when θ >> B. The functions are assumed for the present purpose to continue out to the far periphery, although the increased cone density near the ora serrata suggests that the sizes in this region need detailed verification for a complete analysis.

Mathematical description of the cone density variation: Sufficient information is now available to provide a mathematical description of the variation in cone density with eccentricity. The basic equation that prevails for two log units over the mid range of eccentricities from 0.2 to 20° (eq. 1) will now be replaced by the assumption of the previous section that the cone density is inversely proportional to the luminous flux impinging on each receptor. It should be noted that the density will be expressed in terms of retinal area, and must therefore take account of the angle of the retina with respect to the incident rays (see Fig. 2). The final function for cone density, d_c, is therefore inversely proportional to luminous flux, F, (from eq. 2), with compensation for the angle of the receptors to the retina. In other words, if the receptor density projected to a plane normal to the incident light is inversely proportional to the luminous flux, then the density on the retina itself will be reduced in proportion to the cosine of the angle of the retina to that normal plane. The equation for receptor density then takes the form

$$d_c \approx \cos(\phi) / F \qquad (7a)$$

where ϕ is the internal angle of the incident light on the retina.

Drasdo and Fowler [7] show that their model agrees with the data of Lotmar [12] in estimating the internal angle to be approximately proportional to the external angle, with a proportionality constant, v, close to that from eq. 3, which was 0.82. Substitution for ϕ from this relation and for F from eq. 2, and the substitution of expressions for cone radius from eq. 6 and receptor illuminance from eqs. 3,4 and 5, results in the full expression for cone density:

$$d_c = \frac{A \cdot \left[1 - w \cdot (1 - \cos(u \cdot \theta))\right]^2}{m_c \cdot (B+\theta)^{0.33}} \qquad (7b)$$

where A is an areal constant of proportionality which includes the 2π term from eq. 2.

This equation represents the final form of the mathematical description of the cone density function, and it has only the density scaling constant, A, as a free parameter. Fig. 5 shows the fit of this function (full line) to the most complete set of data, close to the horizontal temporal (0°) meridian from Fig. 1. The value of the scaling constant, A, was 30,000 cones/mm^2.

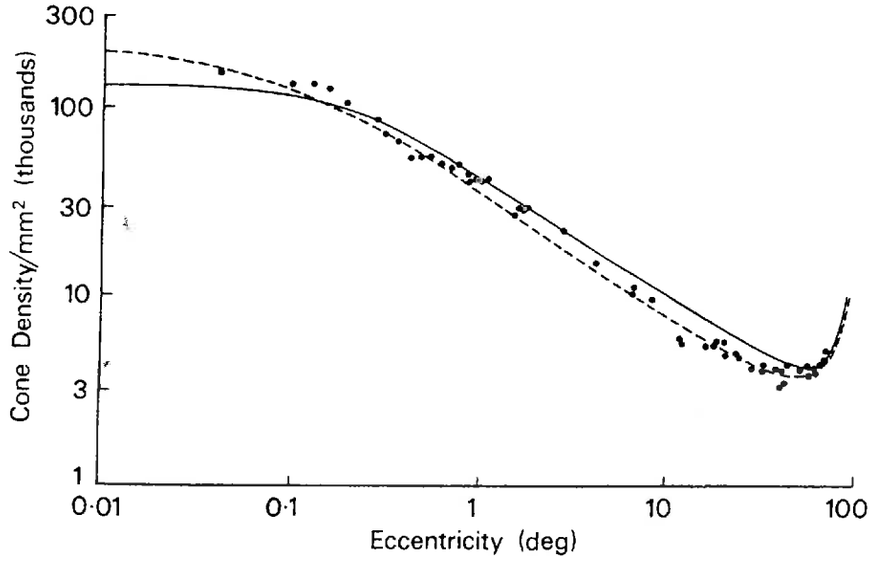

Fig. 5. Fit of function in eq. 6 (full line) to cone densities near the horizontal temporal (0°) meridian, based on the principle of compensation for integrated luminous flux at the receptors, with no free parameters other than a vertical scaling constant. Dashed line shows improved fit obtained by assuming an eccentricity constant of 5' for the foveolar singularity.

Equation 6 provides a good fit to the cone density data across the full range of eccentricities, although it is slightly low in the foveola and somewhat high in the mid periphery for the temporal data.

In the midrange of eccentricities, where θ >> B, the cone density is governed by the power law of the cone inner segment areas with a slope of -0.33 x 2 or -0.66, close to the empirical value of -0.63 found from eq. 1. A slight reduction is to be

expected from the asymptotic behavior at the two extremes. Note also that the deviation from the basic power law provided by the cosine terms gives an excellent description of the upturn in the far periphery, again with no free parameters. The steep portion beyond the range of the temporal data shows the increase of up to a factor of 3 above the mid-peripheral densities required to fit the other data sets in Fig. 1.

To show that the present approach is capable of completely fitting the data with a little extra freedom in the parameters, the dashed line in Fig. 5 gives a second solution to eq. 6 assuming a different eccentricity constant of 0.080 (5') for Polyak's data [8] (which are not well determined in the foveola), smaller by a factor of 2.5 than the best fitting value. The function was then rescaled to a density of 36,500 at the center but all other parameters relating to the receptor illuminance hypothesis were the same. With this small adjustment the function now fits the cone density data within the error of estimation of 0.1 log units for each point.

Conclusion

The densities and sizes of receptors in the human retina show a remarkable degree of regularity in their variation with eccentricity. A few straightforward equations suffice to describe their behavior throughout the retina. Over most of the useful visual range outside the foveal singularity, both cone sizes and cone densities can adequately be described by power functions with specific exponents which differ from unity (eqs. 1, 5, and 6). Given the function of cone size variation, the cone density can be predicted directly on the basis of a hypothesis of compensation for receptor illuminance. This type of analytic anatomy is suggestive of relatively simple ontogenetic principles in the development of the retina.

Acknowledgments:

My thanks to Gerald Silverman for extensive data processing and to Stanley Schein for helpful discussion. Supported by NSF BNS 8711217 and NIH grant RR 5566.

References

1. Oesterberg GA. Topography of the layer of rods and cones in the human retina. Acta Ophthal Suppl VI 1935.
2. Curcio CA, Sloan KR, Packer O, Hendrickson AE, Kalina RE. Distribution of cones in human and monkey retina: Individual variability and radial asymmetry. Science 1987;236:579-582.
3. Schein S.J. Anatomy of macaque fovea and spatial densities of neurons in foveal representation. J Comp Neurol 1988;269:479-505.
4. Williams RW. The human retina has a cone-enriched rim. Vis Neurosci 1991;6:403-406.
5. Spring KH, Stiles WS. Apparent shape and size of the pupil viewed obliquely. Br J Ophth 1948;32:347-354.
6. Jay BS. Effective pupillary area at varying perimetric angles. Vision Res 1962;1:418-24.
7. Drasdo N, Fowler CW. Non-linear projection of the retinal image in a wide-angle schematic eye. Br J Ophth 1974; 58:709-714.
8. Polyak S. The retina. Chicago: University of Chicago Press 1941.
9. Laties AM, Liebmann PA, Campbell CEM. Photoreceptor orientation in the primate eye. Nature 1968;218: 172-173.
10. Charman WN. The retinal image in the human eye. In: Osborne NN, Chader GJ, editors. Progress in retinal research. Oxford: Pergamon Press, 1983: 1-50.
11. Tyler CW. Analysis of visual modulation sensitivity II. Peripheral retina and the role of photoreceptor dimensions. J Opt Soc Am A 1985;2:393-398.
12. Lotmar W. Theoretical eye model with aspherics. J Opt Soc Am 1971;61:1522-1529.